EBioMedicine 38 (2018) 238–247

Contents lists available at ScienceDirect

EBioMedicine

journal homepage: www.ebiomedicine.com

EBioMedicine
Published by THE LANCET

Research paper

Evaluation of the antifibrotic potency by knocking down SPARC, CCR2 and SMAD3

Weifeng Ding [a,b,g,1], Weilin Pu [a,1], Shuai Jiang [a], Yanyun Ma [a], Qingmei Liu [c], Wenyu Wu [c], Haiyan Chu [a], Hejian Zou [d,e], Li Jin [a,f], Jiucun Wang [a,c,e,f,**], Xiaodong Zhou [g,*]

[a] State Key Laboratory of Genetic Engineering, Collaborative Innovation Center for Genetics and Development, School of Life Sciences, Fudan University, Shanghai, China
[b] Department of Laboratory Medicine, Affiliated Hospital of Nantong University, Nantong, Jiangsu Province, China
[c] Department of Dermatology, Huashan Hospital, Fudan University, Shanghai, China
[d] Division of Rheumatology, Huashan Hospital, Fudan University, Shanghai, China
[e] Institute of Rheumatology, Immunology and Allergy, Fudan University, Shanghai, China
[f] Human Phenome Institute, Fudan University, Shanghai, China
[g] University of Texas-McGovern Medical School, Houston, TX, USA

ARTICLE INFO

Article history:
Received 10 August 2018
Received in revised form 23 October 2018
Accepted 9 November 2018
Available online 20 November 2018

Keywords:
Fibrosis
Multiple targets-siRNAs
SPARC
SMAD3
CCR2
Inflammation
Peptide nanoparticle
Scleroderma

ABSTRACT

Background: The genes of SPARC, CCR2, and SMAD3 are implicated in orchestrating inflammatory response that leads to fibrosis in scleroderma and other fibrotic disorders. The aim of the studies is to evaluate synergistic anti-fibrotic potency of the siRNAs of these genes.
Methods: The efficacy of the siRNA-combination was evaluated in bleomycin-induced mouse fibrosis. The pathological changes of skin and lungs of the mice were assessed by hematoxylin and eosin and Masson's trichrome stains. The expression of inflammation and fibrosis associated genes and proteins in the tissues were assessed by real-time RT-PCR, RNA sequencing, Western blots and ELISA. Non-crosslinked fibrillar collagen was measured by the Sircol colorimetric assay.
Findings: The applications of the combined siRNAs in bleomycin-induced mice achieved favorable anti-inflammatory and anti-fibrotic effects. Activation of fibroblasts was suppressed in parallel with inhibition of inflammation evidenced by reduced inflammatory cells and proinflammatory cytokines in the BALF and/or the tissues by the treatment. Aberrant expression of the genes normally expressed in fibroblasts, monocytes/macrophage, endothelial and epithelial cells were significantly restrained after the treatment. In addition, transcriptome profiles indicated that some bleomycin-induced alterations of multiple biological pathways were recovered to varying degrees by the treatment.
Interpretation: The application of the combined siRNAs of SPARC, CCR2, and SMAD3 genes ameliorated inflammation and fibrosis in bleomycin-induced mice. It systemically reinstated multiple biopathways, probably through controlling on different cell types including fibroblasts, monocytes/macrophages, endothelial cells and others. The multi-target-combined therapeutic approach examined herein may represent a novel and effective therapy for fibrosis.

1. Introduction

Systemic fibrosis, such as systemic sclerosis (SSc), is often a fetal disease [1]. In US, among the lethal consequence caused by different diseases, the proportion of the fibrosis takes up about 45% [2]. Although various anti-inflammatory, anti-fibrotic and immunosuppressive agents are used to control fibrosis, majority of them have not been proven successful [1,3,4]. Therefore, developing novel anti-fibrotic intervention is urgently needed. Pathological prototype of many systemic fibrotic disorders is characterized by excessive extracellular matrix (ECM), inflammation, abnormal immunity and vasculopathy, which are mainly

* Corresponding author at: University of Texas-McGovern Medical School, TX, USA.
** Correspondence to: Jiucun Wang, School of Life Sciences and Huashan Hospital, Fudan University, Shanghai, China.
E-mail addresses: jcwang@fudan.edu.cn (J. Wang), xiaodong.zhou@uth.tmc.edu (X. Zhou).
[1] These authors contributed equally to the manuscript.

https://doi.org/10.1016/j.ebiom.2018.11.016

Research in context

Evidence before this study

Systemic fibrosis, such as systemic sclerosis (SSc), is often a fetal disease. In US, among the lethal consequence caused by different diseases, the proportion of the fibrosis takes up about 45%. Although various anti-inflammatory, anti-fibrotic and immunosuppressive agents are used to control fibrosis, majority of them have not been proven successful. Therefore, developing novel anti-fibrotic intervention is urgently needed. Mounting evidences have demonstrated that the genes of SPARC, CCR2, and SMAD3 are implicated in orchestrating inflammation and fibrosis in scleroderma and other fibrotic disorders. Our previous research had demonstrated SPARC inhibition attenuated fibrosis in vitro and in vivo. Moreover, other reports had verified that blockade of CCR2 ameliorates progressive fibrosis in lung and kidney via suppressing macrophage infiltration and activation. And the $Smad3^{-/-}$ mice are protected against renal tubule-interstitial fibrosis by blocking of endothelial mesenchymal transition (EMT) and abrogation of monocyte influx and collagen accumulation. Overall, SPARC, CCR2, and SMAD3 are three important molecules expressed in various cell types, and they have been implicated in orchestrating the fibrotic response. Traditional strategy of anti-fibrosis is to target single gene, which may limit its impact to fibrosis that usually involves comprehensive bio-networks conducted by different cell types. However, a multi-target therapeutic approach may systemically reinstate multiple biopathways involved in inflammation and fibrosis.

Added value of this study

For human complex diseases, like systemic sclerosis (SSc), targeting on an individual molecule may be insufficient to restore the healthy state. Modulating the activity of multiple targets might achieve optimal therapeutic benefit. Our selected three target genes have been well-documented as critical players contributing to multiple cellular biopathways in SSc. Our results indicated that the combination of siRNAs targeting on these genes achieved favorable anti-inflammatory and anti-fibrotic effects with a systemic improvement at cellular and molecular levels. This article represents the first attempt to apply multi-target treatment in a fibrotic mouse model that involves complex cellular and molecular pathways leading to inflammation and fibrosis. It provides supportive evidence for a potentially radical shift of therapeutic strategy from current single- to multiple-targets approach in SSc and other human complex diseases.

Implications of all the available evidence

Taken together, inhibition of the triple-target genes attenuated inflammation and/or fibrosis in both lung and skin tissues of the mouse models. Inhibition of inflammation was evidenced by reduced inflammatory cells and proinflammatory cytokines in the bronchoalveolar lavage fluid and/or the tissues. Underlying morphologic improvement of mouse tissues, activation of fibroblasts was suppressed in mouse tissues in which α-Sma (alpha smooth muscle actin) and collagens were significantly reduced.
Importantly, aberrant expressions of some genes involved in functions of fibroblasts, monocytes/ macrophage, endothelial and epithelial cells were reinstalled after the treatment. In addition, transcriptome profiles indicated that some bleomycin-induced alterations of multiple biological psathways were recovered to varying degrees by the treatment. A systemic effect of the triple-target treatment involves not only fibrosis, but also multiple other biological cascades, such as metabolism, oxidative phosphorylation, et al. Therefore, the multi-target therapeutic approach examined herein may represent a novel and effective therapy for systemic fibrosis.

involved in fibroblast, monocytes, lymphocytes and endothelium, as well as the interaction among these different cell types [1,3].

SPARC (secreted protein, acidic and rich in cysteine) is a matricellular component of ECM mainly expressed by fibroblasts, endothelial cells and lipocytes [5,6]. It is an important mediator of cell-matrix interaction [7]. It is commonly overexpressed in fibrotic tissue [6,8–11]. SPARC can stimulate canonical transforming growth factor (TGF)-β pathway [12,13], and it also plays a possible role in the recruitment of neutrophils to the sites of acute inflammation [14]. Our previous research had demonstrated SPARC inhibition attenuated fibrosis in vitro and in vivo [15].

CCR2 (C—C chemokine receptor 2) is a common receptor of monocyte chemoattractant proteins (MCP 1, 2, 3, 4 and 5) [16], and it is normally expressed on monocytes, as well as activated T cells, B cells and immature dendritic cells [17,18]. It not only directs the recruitment of immune cells to the sites of inflammation, but is also involved in angiogenesis, development of fibrosis, migration of fibrocytes to the alveolar space after fibrotic injury [19]. CCR2 and its ligands (MCP1 and MCP3) are highly expressed in SSc-related fibrotic tissues [20]. Blockade of CCR2 ameliorates progressive fibrosis in lung and kidney via suppressing macrophage infiltration and activation [21].

The SMADs (Drosophila mothers against decapentaplegic proteins) are a family of intracellular molecules that act as the main TGF-β signal transducers [22]. As an important member of R-SMADs (receptor-regulatory SMADs), SMAD3 is normally expressed in epithelial cells and lymphocytes [23,24], and possible other type of cells (e.g. fibroblasts) under disease status or upon TGF-β activation [25]. TGF-β/SMAD signaling plays crucial roles in immune dysregulation, secretion of inflammatory and fibrogenic cytokines and chemokines, and fibroblast activation [26–28]. The $Smad3^{-/-}$mice are protected against renal tubule-interstitial fibrosis by blocking of endothelial mesenchymal transition (EMT) and abrogation of monocyte influx and collagen accumulation [28].

Overall, SPARC, CCR2, and SMAD3 are three important molecules expressed in various cell types, and they have been implicated in orchestrating the fibrotic response. The studies herein applied the siRNAs of these three genes to examine a multi-target therapeutic approach that may systemically reinstate multiple biopathways involved in inflammation and fibrosis of the mouse model of fibrosis.

2. Materials and methods

2.1. siRNAs

Mouse siRNAs for Sparc and Ccr2 were synthesized by Gene Pharma Inc. (Shanghai, China) and Ribobio Inc. (Guangzhou, China), respectively. Mouse Smad3 Trilencer-27 siRNAs and non-target siRNAs were purchased from Origene Inc. (Rochville, MD, USA). To avoid off-target effect, two pairs of each target gene siRNAs were utilized, and both of them knockdowned their targeted genes but did not impact the mRNA levels of the housekeeping gene, *Gapdh* in a mouse embryo fibroblast NIH 3 T3 cell line (Supplementary Fig. S1).

2.2. Animal models of pulmonary fibrosis, delivery of combined siRNAs in vivo

Female C57BL/6 mice of about 20 g were purchased from SLRC laboratory animal Inc. (Shanghai, China). Pulmonary fibrosis model was

induced by intratracheal instillation of 3 mg/kg bleomycin (BLM, Nippon Kayaku Co., Tokyo, Japan) for one time [29]. A total of 5.6 μg combined siRNAs for Sparc, Ccr2 and Smad3 encapsulated by peptide nanoparticles (PNP) [30] were injected intraperitoneally with 130 μl PBS on day 10, 14, 18 after BLM induction (Supplementary Fig. S2). All groups of mice were sacrificed on day 22 after anesthesia, and the bronchoalveolar lavage fluid (BALF) and the lung samples were collected. The left lungs were ligated for the extraction of BALF, then fixed with 4% formalin and used for further histological analysis. The right lung tissues were divided into three parts, one for RNA extraction, another one for collagen content analysis, the rest for western blot detection.

2.3. Animal models of dermal fibrosis, delivery of combined siRNAs in vivo

For dermal fibrosis model, female C57BL/6 mice about 5 weeks old were induced by the local subcutaneous injection of 100 μl BLM (0.5 mg/ml) per day in the shaved lower back for three weeks. The treatments were performed by subcutaneous injection to lower back of 3 μg of combined siRNAs and PNP on day 7, 10, 12, 14, 16, 18, 20 after three hours of BLM administration (Supplementary Fig. S3). All of the mice were sacrificed on day 22 and the skin samples were collected. Five mice were examined in saline group, BLM group, Nano (BLM + PNP) group and therapeutic group, respectively. Saline injections were used as negative controls in both lung and skin fibrosis models. The animal protocols were approved by the Center of Laboratory Animal Medicine and Care of Fudan University.

2.4. Determination of gene expression by quantitative RT-PCR

See Supplementary Materials and Methods.

2.5. Detection of protein level by Western blot

See Supplementary Materials and Methods.

2.6. Histological analysis

See Supplementary Materials and Methods.

2.7. Total and differential nucleated cell count in the BALF

See Supplementary Materials and Methods.

2.8. Determination of concentration of cell factor by ELISA

See Supplementary Materials and Methods.

2.9. Determination of soluble collagen content

Non-crosslinked fibrillar collagen in lung and skin samples was measured by the Sircol colorimetric assay (Biocolor, Belfast, UK). Minced tissues were homogenized in 0.5 M acetic acid with about 1:10 ratio of pepsin (Sigma, USA). Tissues were weighted and incubated overnight at 4 °C with vigorously stirring. Digested samples were centrifuged and the supernatant was used for Sircol dyeing to detect the collagen content. The total protein concentration was determined by using Bradford protein assay kit (Abcam) and the collagen content of each sample was normalized to total protein.

2.10. RNA sequencing assay to evaluate the anti-fibrotic effect of multi-genes siRNAs in pulmonary fibrosis mouse models

Total RNA was extracted and used to construct the cDNA library with a KAPA RNA HyperPrep kit (Kapa biosystems, Wilmington, Massachusetts, USA) according to the manufacturer's instruction. Then the cDNA libraries were sequenced by Illumina HiSeq X Ten systems (Illumina, USA). The average sequencing depth of each fragment was 140 X. The transcriptome data was analyzed with the tophat 2 and cufflinks pipeline according to the instructions.

2.11. Statistical analysis

One-way ANOVA (analysis of variance) was used to analyze the difference of multi-groups in treatment. Unpaired *t*-test with welch's correction was used to test the significance between two groups. A p-value of <0.05 was considered as statistical significance.

3. Results

3.1. PNP/PRSsi ameliorated fibrosis in lungs tissues induced by BLM

Low toxicity, high efficiency and low off-target rates of the peptide nanoparticles (PNP, Supplementary Fig. S4) were observed and consistent with the previous report [30]. The expression levels of the targeted genes including *Sparc*, *Ccr2* and *Smad3* were decreased significantly in the therapeutic groups (Supplementary Fig. S5-S6). In parallel, the expression levels of *Col1a1* of the lung tissues were significantly reduced in the treatment group with triple siRNAs for SPARC (P), CCR2 (R), and SMAD3 (S) carried by the PNP (PNP/PRSsi) compared to that in Nano (BLM + PNP) groups, and showed considerable but no statistical significance reduction of *Col1a1* compared with BLM group. Meanwhile, the expression level of *Col3a1* was significantly down-regulated in PNP/PRSsi group compared to both BLM and Nano groups (Fig. 1A). Moreover, the protein level of type I collagen (Fig. 1C and D) and the soluble collagen content (Fig. 1B) were significantly reduced in the PNP/PRSsi treatment groups compared to those in BLM and Nano groups. The HE (Fig. 1E upper) and Masson Trichrome (Fig. 1E lower) staining showed that the BLM or Nano group had thicker collagen-fiber in the impaired lung alveolar wall compared to those in the saline-injection and the treatment groups. After PNP/PRSsi treatments, only a small quantity of the collagen-fiber was found and the tissue architecture of the lung alveolar was relatively intact (Fig. 1E). Moreover, the Ashcroft score of the mice in PNP/PRSsi treatment group is significantly reduced compared to that in the BLM and Nano group (Supplementary Fig. S7). These results indicated that the pulmonary fibrosis was significantly alleviated by PNP/PRSsi treatments in the BLM-induced mice.

3.2. PNP/PRSsi antagonized fibrosis in skin tissues induced by BLM

The treatment with PNP/PRSsi significantly reduced the skin *Col1a1* and *α-SMA* (alpha smooth muscle actin) mRNA expression. In addition, the expression of *Col1a2* and *Col3a1* were both considerably down-regulated, but that did not reach the statistical significance in the PNP/PRSsi treatment group compared to the BLM and Nano groups (Fig. 2A). Moreover, type I collagen protein level was also significantly reduced compared to those in the BLM and Nano groups (Fig. 2B and C). The soluble collagen content in skin tissues of the mice was also significantly decreased in the therapeutic group (Fig. 2D). On contrast, *Mmp3* (matrix metalloproteinase 3) mRNA expression (Fig. 2E) was remarkably up-regulated in the PNP/PRSsi treatment group. Furthermore, the thickness of the dermis was significantly reduced in the therapeutic groups compared to that in the BLM and Nano groups (Supplementary Fig. S8). Meanwhile, the PNP/PRSsi treatment also decreased collagen-fiber bundles and reduced fat tissue in dermal skin compared to that in the BLM and Nano groups by HE and Trichrome staining (Fig. 2F). In addition, the number of detectable capillaries per 100-fold power lens in the dermal skin was significantly increased in the PNP/PRSsi treatment group compared to that in the BLM or Nano groups (Supplementary Fig. S9).

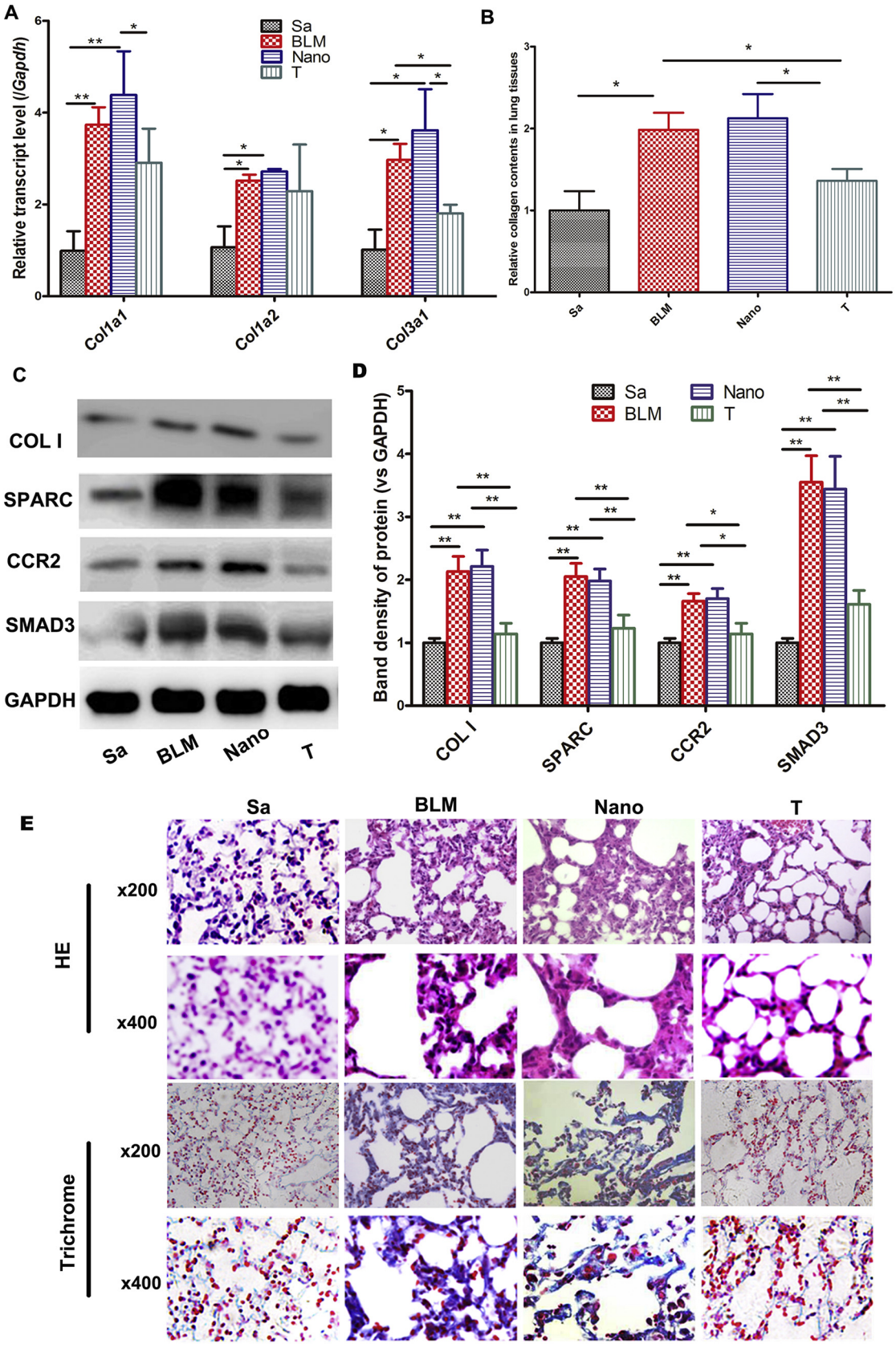

Fig. 1. Examination of the anti-fibrotic effect in lungs of mouse models induced by bleomycin ($n = 4$) (A) The mRNA levels of collagen *Col1a1*, *Col1a2*, and *Col3a1* were examined by Q-PCR. (B) Sircol assays to detect the soluble collagen content in the pulmonary tissues. (C) The type I collagen protein was detected by western blotting. COL I: type I collagen protein of the mouse. (D) The protein density in lung tissues was quantified by the Image-QuantTL software (General Electric Company, CT, USA). (E) Representative histological figures of HE and Trichrome staining of mouse lung tissues in the different groups. Sa: saline group, injected with saline (negative control); BLM: BLM group, injection with BLM only on day 0; Nano: Nano group, injection with BLM and PNP; T: therapeutic group, injection with PNP/PRSsi; *: $P < .05$ and **: $P < .01$.

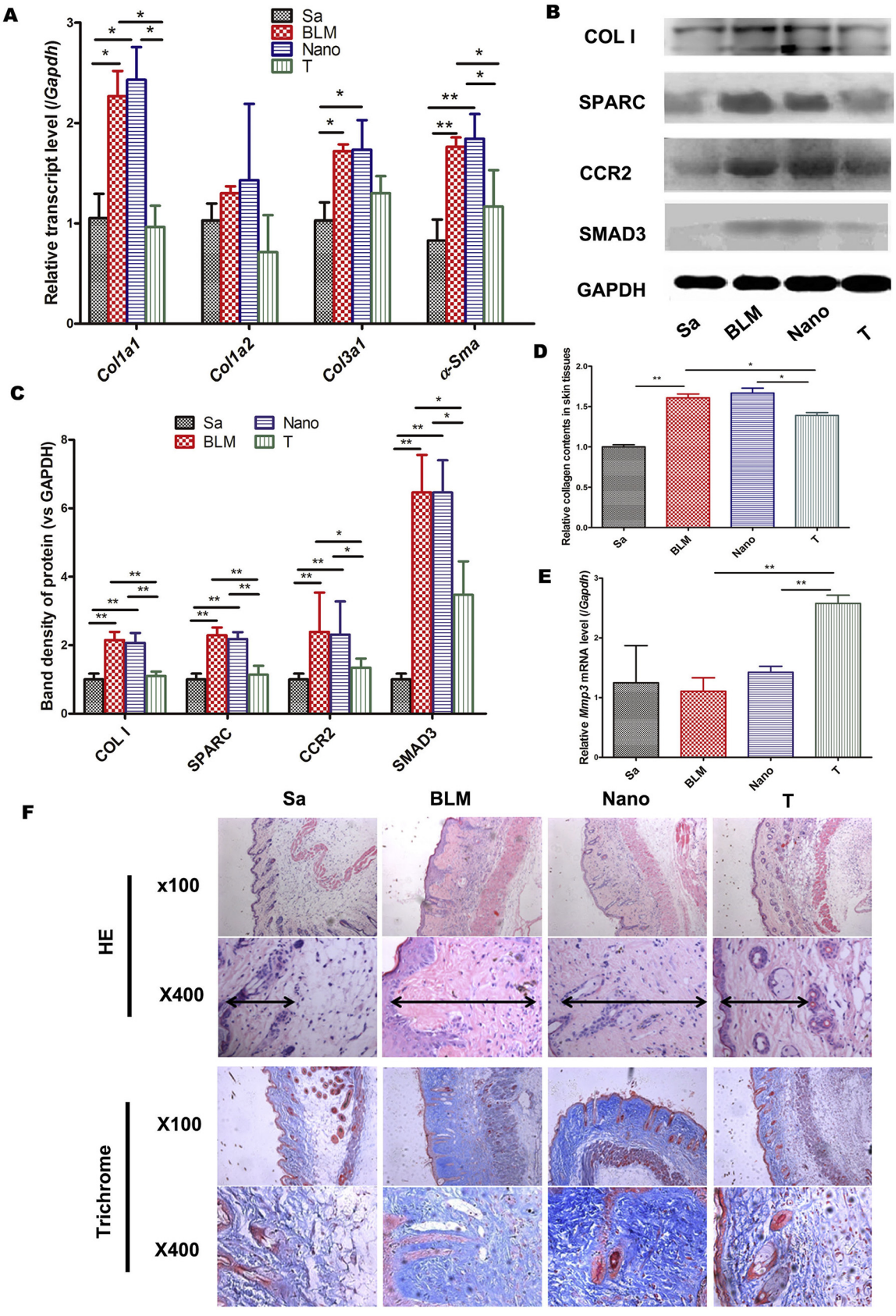

Fig. 2. Examination of the anti-fibrotic effect in skin of mouse models induced by bleomycin ($n = 5$) (A) The mRNA levels of collagen *Col1a1*, *Col1a2*, *Col3a1*, and *α-SMA* were examined by Q-PCR. (B) Collagen I protein was detected by western blotting. (C) The protein density in skin tissues was quantified by the Image-QuantTL software. (D) Sircol assays to detect the soluble collagen content in the skin tissues. (E) The mRNA expression level of the anti-fibrotic gene, *Mmp3* was examined by Q-PCR. (F) Representative histological figures of HE and Trichrome staining of mouse skin samples in the different groups. Sa: saline group, injected with saline; BLM: BLM group, injection with BLM per day from day 0 to day 21; Nano: Nano group, injection with BLM and PNP per day; T: treatment group, injection with PNP/PRSsi treatments. *: $P < .05$ and **: $P < .01$. Di-arrowhead indicated the thickness of the dermis.

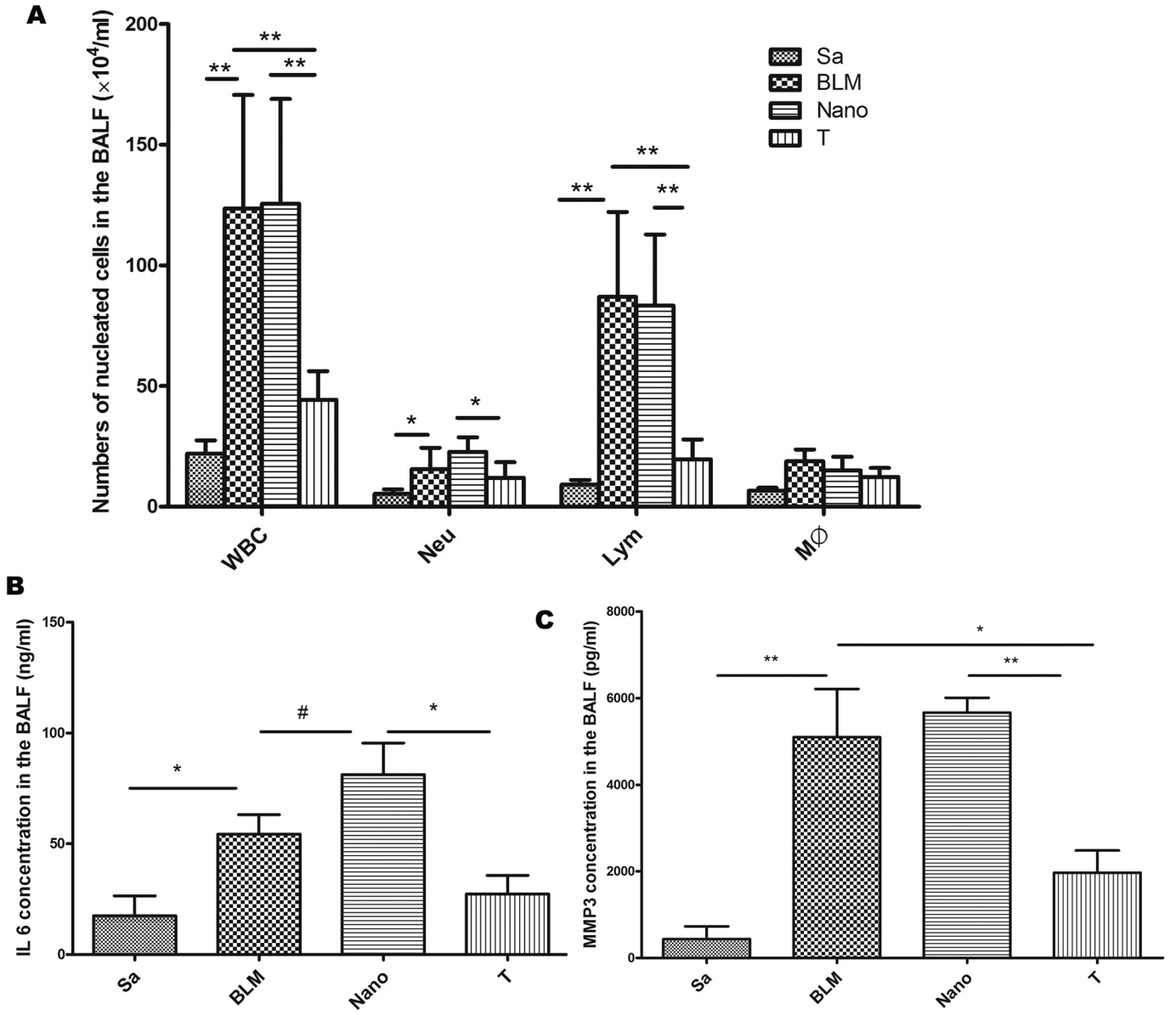

Fig. 3. Examination of the inflammatory cells and inflammatory cytokines in the BALF of pulmonary fibrosis mouse models (n = 4) (A) White blood cells count and differential count by Wright-Giemsa's staining in the BALF under the optical microscope. The concentration of IL 6 (B) and MMP3 (C) proteins in the BALF were detected by ELISA. Sa: injected with saline (negative control); BLM: injection with BLM only on day 0; Nano: injection with BLM and PNP; T: therapeutic treatments; WBC, white cells count; Neu, neutrophil; Lym, lymphocyte; Mϕ, macrophage. *: $P < .05$ and **: $P < .01$. #, $P > .05$.

3.3. PNP/PRSsi reduced inflammation in the BALF of mouse models with pulmonary fibrosis

The total number of inflammatory cells along with the MMP3 level were significantly reduced in the bronchoalveolar lavage fluid (BALF) of the mice in the treatment group compared to that in both the BLM and Nano groups (Fig. 3A, C and Table 1). The IL-6 level was decreased by about 50% with marginally significantly ($p = .084$) (Fig. 3B).

3.4. PNP/PRSsi attenuated inflammation and immune response in lung and skin fibrosis mouse models

In the mice with pulmonary fibrosis, compared to the BLM and Nano groups, the expression levels of *Il-6 and Mmp3 genes* were remarkably reduced in the treatment groups (Fig. 4A, E). On the other hand, the expression level of *Ifn-γ*, a cytokine with anti-fibrotic activity [31,32] was up-regulated in the treatment group (Fig. 4B). In the mice with skin fibrosis, an increase of mRNA levels of *Ifn-γ* (Fig. 4C) and *Il-10* (Fig. 4D) were observed in the treatment group. It implied that PNP/PRSsi could attenuate pro-inflammatory cytokines and also mediated the immunity response via cytokine IL 10 to inhibit fibrosis.

Table 1
The percentage of nucleated cells in the BALF.

Cell count(%)	Sa	BLM	Nano	T
Neu (%)	23.2 ± 3.66	12.7 ± 7.22	20.0 ± 5.73	23.7 ± 11.88
Lym (%)	42.7 ± 3.66	68.3 ± 5.51	65.6 ± 2.06	41.0 ± 11.07*
Mac (%)	31.2 ± 3.36	17.0 ± 5.42	12.3 ± 1.91	34.1 ± 21.81

* : $P < .05$ between the T VS BLM or Nano group. Sa: injected with saline (negative control); BLM: injection with BLM only on day 0; Nano: injection with BLM and PNP; T: therapeutic treatments; Neu: neutrophil; Lym: lymphocyte; Mac: macrophage.

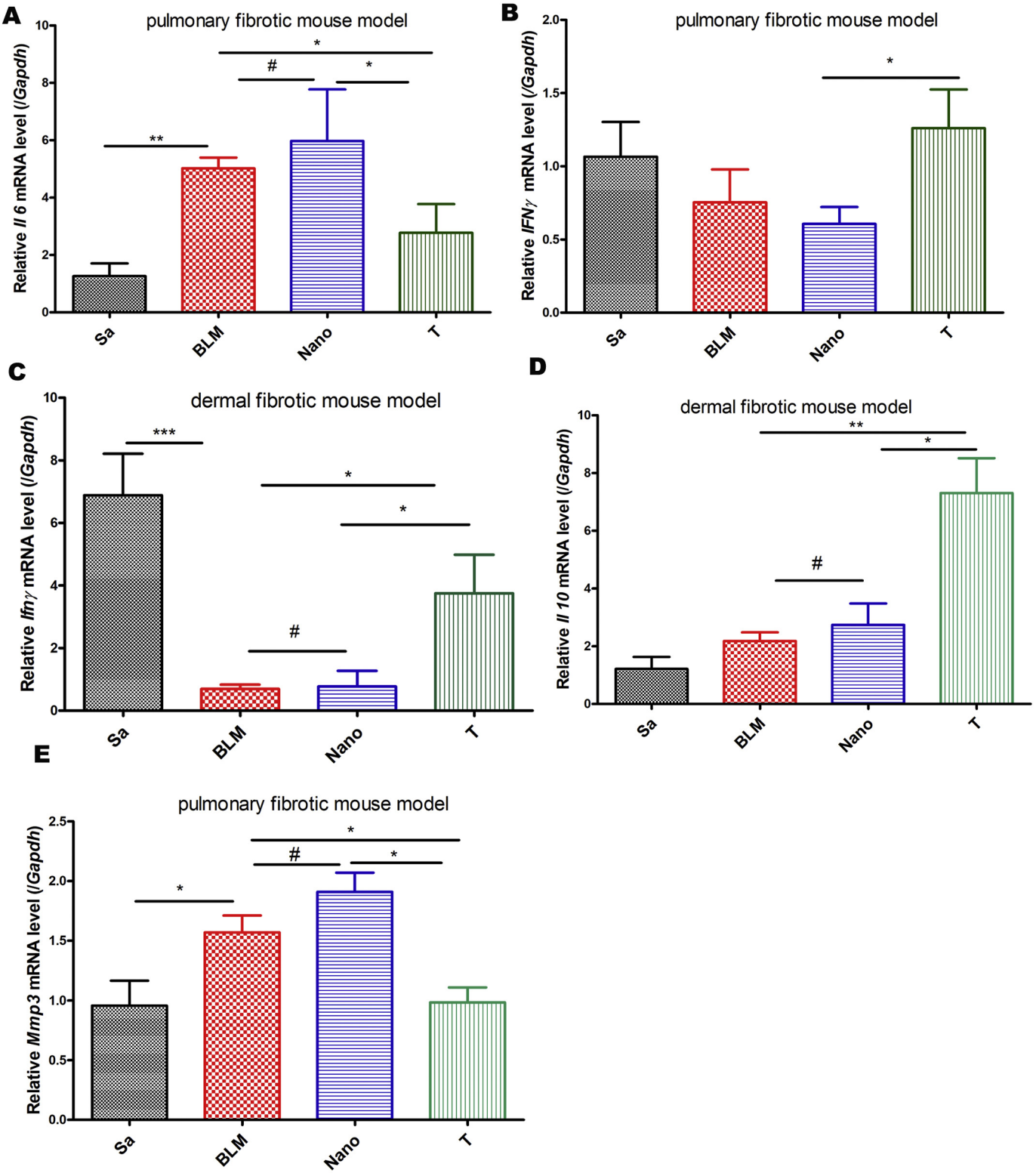

Fig. 4. Examination of the cytokines involved in the inflammation and immune response in dermal and pulmonary mouse models by Q-PCR (A) *Il 6* and (E) *Mmp3* mRNA levels were examined in pulmonary fibrosis mouse models. (B, C) *Ifn γ* mRNA levels were examined in lung and skin fibrosis models, respectively. (D) *Il 10* mRNA levels were examined in dermal fibrosis mouse models. Sa: injected with saline (negative control); BLM: injection with BLM; Nano: injection with BLM and PNP; T: therapeutic treatments. *: $P < .05$, **: $P < .01$, ***: $P < .001$, #: $P > .05$.

3.5. Gene expression profiles validated the anti-fibrosis effect of PNP/PRSsi in pulmonary model

The heatmap of RNA sequencing based on all of the variable genes showed that the gene expression patterns were similar between the saline and PNP/PRSsi treatment groups (Fig. 5A). There were 156 DEGs (differentially expressed genes) between BLM and PNP/PRSsi treatment groups, and 1397 DEGs between BLM and saline treatment groups. Among these 1553 DEGs, 103 genes were shared (Fig. 5C). These shared DEGs were mainly involved in Notch signaling (e.g.

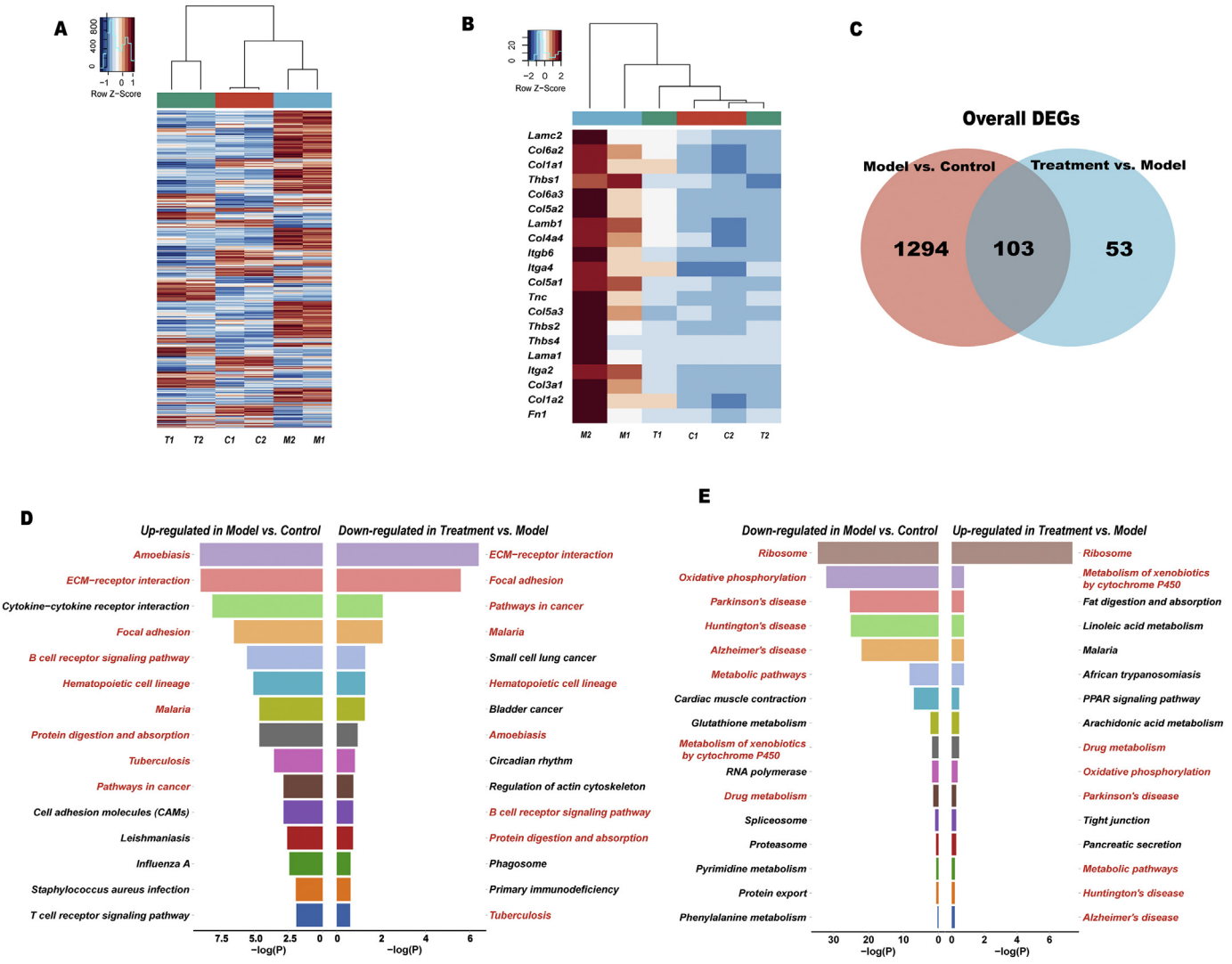

Fig. 5. The gene expression profiles in the control, model and PNP/PRSsi treatment mice in pulmonary fibrosis mouse models. (A) The heatmap of all the differentially expressed genes (DEGs) among the control, model and treatment groups. Horizontal axis was depicted as a z score of each gene expression level with FPKM (fragments per kilobase of transcript per million fragments mapped). Vertical axis represents each of the DEGs. C: Saline group that the mouse models were injected with saline and served as the negative control, M: the mouse model injected with BLM, which served as a model group, T: the mouse model of treatment group, therapeutic injection with PNP/PRSsi. (B) The expression profiles of DEGs in the extracellular matrix (ECM) pathway among three groups were shown. (C) The Venn diagram showed the unique and shared numbers of the DEGs in different comparisons. 1294 DEGs were unique in the comparison between model group and control group, while 53 DEGs were unique in the comparison between PNP/PRSsi treatment group and model group. Meanwhile, 103 DEGs were shared between the two comparisons. (D) Top 15 significant pathways in KEGG enrichment analysis based on DEGs of different comparisons. Right part represents the down-regulated signaling pathways in the treatment group compared with those of in the model group, while the left part represented the up-regulated signaling pathways in model group compared with those in control group. (E) Top 15 down-regulated pathways in BLM group while partly up-regulated in PNP/PRSsi treatment group.

Notch3, Bcl9l), nuclear receptor signaling (e.g. Rpl39), inflammation (e.g. Mmp9, Ccr5, Mgst1), the SUMO modification (e.g. Sumo1, Ildr2), NOS/hypoxia signaling (e.g. Itga2, Fn1, Ndufa6, Cox6a2), and Toll-like receptor (TLR) pathways (e.g. Tlr9, Oas3) [3,28,33–36]. Some of the genes including Notch3, Mmp9, Ildr2, Sumo1, Rpl39, and Ndufa6 also altered in human lung biopsy samples of pulmonary fibrosis with the similar tendency to that in our mouse models, data from GEO database (Supplementary Fig. S10–15).

The KEGG enrichment analysis revealed most significantly altered biopathways in each comparison of different groups. In particular, the expression pattern of the genes involved in ECM-receptor interaction pathway was significantly up-regulated in BLM group compared with the saline group, and was then significantly retrieve to normal status after PNP/PRSsi treatment (Fig. 5B). The expression profiles of the genes involved in cell adhesion molecules (CAMs) and inflammation-related signaling pathways, including chemokine, NF-κB, and JAK-STAT signaling pathways also showed similar tendency (Supplementary Fig. S16-S17). By contrast, there were 25 genes involved in oxidative phosphorylation and xenobiotics, glutathione metabolic pathways, which were down-regulated in the BLM group, were almost revived to the normal status after PNP/PRSsi treatments (Supplementary Fig. S18).

Other top up-regulated gene clusters (e.g. cytokine-cytokine receptor interaction, B cell receptor, protein digestion and absorption) and down-regulated ones (e.g. metabolic pathways, ribosome, cytochrome *p*450, and drug metabolism in BLM group tended to be balanced by PNP/PRSsi treatment (Fig. 5D and E).

Taken together, the RNA-Seq data indicated that systemic changes of biopathways induced by the BLM were largely recovered by the PNP/PRSsi treatment.

4. Discussion

Traditional strategy of anti-fibrosis is to target single gene. However, the target gene is often specific to single biopathway and cell type expression, which may limit its impact to fibrosis that usually involves comprehensive bio-networks conducted by different cell types. In this

study, we explored a multi-gene-target approach against fibrosis in BLM-induced mouse model. The three targeted genes are distinct in their primary expressing cells. SPARC is mainly expressed in fibroblast and endothelial cells in which it participates in both TGF-β dependent and independent fibrotic pathways [5,6,37], CCR2 in monocyte and lymphocyte involving in inflammatory signaling [17–19], and SMAD3 in lymphocyte and epithelial cells driving canonical TGF-β pathway [23,24].These different cell types and pathways are believed to synergistically contribute to systemic fibrotic process, such as in SSc [3,34,36,38,39]. It is worth noting that like many fibrosis in human diseases, BLM-induced fibrosis in mouse models is TGF-β dependent and inflammation driven process [29,40,41].

As a result, inhibition of these three target genes attenuated fibrosis in both lung and skin tissues induced by BLM. Underlying molecular changes indicated that the activation of fibroblasts was suppressed as the expression of α-Sma and collagen genes (Fig. 1, Fig. 2, and Supplementary Fig. S19) were generally controlled by the PNP/PRSsi treatment. This improvement appeared in parallel with suppression of inflammation evidenced by reduced inflammatory cells and pro-inflammatory cytokines in the BALF and/or the tissues (Fig. 3 and Fig. 4). While monocytes/macrophage are driven force in inflammation, the CCR2 gene along with other inflammatory genes, such as Chi3l3 and Il1rap, commonly expressed by monocytes/macrophage [42] were significantly restrained after the PNP/PRSsi treatment (Supplementary Fig. S20A). On the other hand, microvasculature in the BLM-induced mouse skin appeared to be improved in the PNP/PRSsi-treated mice as the number of detectable capillaries was significantly increased compared to that in the untreated ones (Supplementary Fig. S9). Some endothelial cell expression genes (e.g. Tie1 and Erg) [43] and the gene of Pecam-1 (CD31) that is associated with endothelial-mesenchymal transition (EndoMT) [44] were under controlled in the treated mice (Supplementary Fig. S20B). In addition, some epithelial cell expressing genes (e.g. Clca1 and Serping1) [45] also were recovered from the aberrant expression in the BLM-induced mice (Supplementary Fig. S20C). Despite of these results, it should be acknowledged that only the single mice model, BLM-induced mice was utilized in the studies and other complementary animal models may be needed for drawing a more robust conclusion of the antifibrotic therapy with the PNP/PRSsi approach.

A global view of gene expression profile with RNA sequencing analysis indicated that some BLM-induced alterations of major biological signaling pathways, such as ECM, cytokine-cytokine receptor interaction, focal adhesion, metabolic, B cell receptor signaling, protein digestion and absorption pathways were recovered to varying degrees by the PNP/PRSsi treatment. This observation suggested that the PRSsi treatment tended to systemically reconstruct the biopathways dysregulated in the BLM-induced mice.

Among the genes examined, the changes of Mmp3 expression appeared contradictory in skin and lung tissues. It was up-regulated in the former, but down in the latter after the treatment. In fact, MMP3 functions in both anti-fibrotic and pro-inflammatory roles. As an important ECM degrading enzyme, it renders crucial roles in connective tissue remodeling [46,47]. On the other hand, it may promote the migration and infiltration of the inflammatory cells [48]. Therefore, it is likely that an increased Mmp3 by the treatment may serve as anti-fibrotic function in skin tissue, while a down-regulation could be an indication of controlled inflammation in the lung tissues.

In summary, the application of the combined siRNAs of SPARC, CCR2, and SMAD3 genes ameliorated fibrosis and inflammation in the BLM-induced mice. It systemically reinstated multiple biopathways, probably through controlling on different cell types including fibroblasts, monocytes/macrophages, endothelial cells and others. Considering human fibrotic disorders usually arise from complex networks involving these major cell types, the multi-target-combined therapeutic approach examined herein may represent a novel and effective therapy for fibrosis.

Acknowledgements

We would like to thank our collaborator, Neil Desai from AADIGEN LLC. (Pacific Palisades, CA, USA) to render the nanoparticles materials.

Declaration of interests

We declared no competing interests to the manuscript.

Funding sources

The work was supported by National Natural Science Founds (grant No. 81328001, No. 31521003, No. 81770066, No. 81470254), Shanghai Municipal Science and Technology Major Project (2017SHZDZX01), International S&T Cooperation Program of China (2013DFA30870), 111 Project (B13016) and US NIH NIAID U01 (1U01AI090909).

Author contributions

All authors are involved in the following contribution to the paper: (1) conception and design the study, or analysis and interpretation of data; (2) drafting the article or revising it critically for important intellectual content; (3) final approval of the version to be published.

Appendix A. Supplementary data

Supplementary data to this article can be found online at https://doi.org/10.1016/j.ebiom.2018.11.016.

References

[1] Ho YY, Lagares D, Tager AM, Kapoor M. Fibrosis–a lethal component of systemic sclerosis. Nat Rev Rheumatol 2014;10:390–402.
[2] Wynn TA. Fibrotic disease and the T(H)1/T(H)2 paradigm. Nat Rev Immunol 2004;4:583–94.
[3] Wynn TA, Ramalingam TR. Mechanisms of fibrosis: therapeutic translation for fibrotic disease. Nat Med 2012;18:1028–40.
[4] Abdelaziz MM, Samman YS, Wali SO, Hamad MM. Treatment of idiopathic pulmonary fibrosis: is there anything new? Respirology 2005;10:284–9.
[5] Hunzelmann N, Hafner M, Anders S, Krieg T, Nischt R. BM-40 (osteonectin, SPARC) is expressed both in the epidermal and in the dermal compartment of adult human skin. J Invest Dermatol 1998;110:122–6.
[6] Inagaki H, Lin KH, Maeda S, Saito T. Osteonectin gene expression in fibrotic liver. Life Sci 1996;58:927–34.
[7] Brekken RA, Sage EH. SPARC, a matricellular protein: at the crossroads of cell-matrix communication. Matrix Biol 2001;19:816–27.
[8] Frizell E, Liu SL, Abraham A, Ozaki I, Eghbali M, Sage EH, et al. Expression of SPARC in normal and fibrotic livers. Hepatology 1995;21:847–54.
[9] Kuhn C, Mason RJ. IMMUNOLOCALIZATION of SPARC, TENASCIN, AND THROMBOSPONDIN IN PULMONARY FIBROSIS. American Journal of Pathology 1995;147:1759–69.
[10] Pichler RH, Hugo C, Shankland SJ, Reed MJ, Bassuk JA, Andoh TF, et al. SPARC is expressed in renal interstitial fibrosis and in renal vascular injury. Kidney Int 1996;50:1978–89.
[11] Blazejewski S, Lebail B, Boussarie L, Blanc JF, Malaval L, Okubo K, et al. Osteonectin (SPARC) expression in human liver and in cultured human liver myofibroblasts. American Journal of Pathology 1997;151:651–7.
[12] Schiemann BJ, Neil JR, Schiemann WP. SPARC inhibits epithelial cell proliferation in part through stimulation of the transforming growth factor-beta-signaling system. Mol Biol Cell 2003;14:3977–88.
[13] Zhou XD, Xiong MM, Tan FK, Guo XJ, Arnett FC. SPARC, an upstream regulator of connective tissue growth factor in response to transforming growth factor ss stimulation. Arthritis Rheum 2006;54:3885–9.
[14] Savani RC, Zhou Z, Arguiri E, Wang S, Vu D, Howe CC, et al. Bleomycin-induced pulmonary injury in mice deficient in SPARC. American Journal of Physiology-Lung Cellular and Molecular Physiology 2000;279:L743–50.
[15] Wang J-C, Lai S, Guo X, Zhang X, de Crombrugghe B, Sonnylal S, et al. Attenuation of fibrosis in vitro and in vivo with SPARC siRNA. Arthritis Res Ther 2010;12.
[16] Carulli MT, Ong VH, Ponticos M, Shiwen X, Abraham DJ, Black CM, et al. Chemokine receptor CCR2 expression by systemic sclerosis fibroblasts: evidence for autocrine regulation of myofibroblast differentiation. Arthritis Rheum 2005;52:3772–82.
[17] Raghu H, Lepus CM, Wang Q, Wong HH, Lingampalli N, Oliviero F, et al. CCL2/CCR2, but not CCL5/CCR5, mediates monocyte recruitment, inflammation and cartilage destruction in osteoarthritis. Ann Rheum Dis 2017;76:914–22.
[18] Sierra-Filardi E, Nieto C, Dominguez-Soto A, Barroso R, Sanchez-Mateos P, Puig-Kroger A, et al. CCL2 shapes macrophage polarization by GM-CSF and M-CSF:

identification of CCL2/CCR2-dependent gene expression profile. J Immunol 2014; 192:3858–67.
[19] Moore BB, Kolodsick JE, Thannickal VJ, Cooke K, Moore TA, Hogaboam C, et al. CCR2-mediated recruitment of fibrocytes to the alveolar space after fibrotic injury. Am J Pathol 2005;166:675–84.
[20] Distler JH, Akhmetshina A, Schett G, Distler O. Monocyte chemoattractant proteins in the pathogenesis of systemic sclerosis. Rheumatology (Oxford) 2009;48:98–103.
[21] Kitagawa K, Wada T, Furuichi K, Hashimoto H, Ishiwata Y, Asano M, et al. Blockade of CCR2 ameliorates progressive fibrosis in kidney. Am J Pathol 2004;165:237–46.
[22] Zerr P, Palumbo-Zerr K, Huang J, Tomcik M, Sumova B, Distler O, et al. Sirt1 regulates canonical TGF-beta signalling to control fibroblast activation and tissue fibrosis. Ann Rheum Dis 2016;75(1):226–33.
[23] Nakao A, Imamura T, Souchelnytskyi S, Kawabata M, Ishisaki A, Oeda E, et al. TGF-beta receptor-mediated signalling through Smad2, Smad3 and Smad4. EMBO J 1997;16:5353–62.
[24] Datto MB, Frederick JP, Pan L, Borton AJ, Zhuang Y, Wang XF. Targeted disruption of Smad3 reveals an essential role in transforming growth factor beta-mediated signal transduction. Mol Cell Biol 1999;19:2495–504.
[25] Kong P, Shinde AV, Su Y, Russo I, Chen B, Saxena A, et al. Opposing Actions of Fibroblast and Cardiomyocyte Smad3 Signaling in the Infarcted Myocardium. Circulation 2018;137:707–24.
[26] Tomcik M, Palumbo-Zerr K, Zerr P, Avouac J, Dees C, Sumova B, et al. S100A4 amplifies TGF-beta-induced fibroblast activation in systemic sclerosis. Annals of the rheumatic diseases; 2014.
[27] Lopez-Sanchez I, Dunkel Y, Roh YS, Mittal Y, De Minicis S, Muranyi A, et al. GIV/Girdin is a central hub for profibrogenic signalling networks during liver fibrosis. Nat Commun 2014;5:4451.
[28] Nanthakumar CB, Hatley RJ, Lemma S, Gauldie J, Marshall RP, Macdonald SJ. Dissecting fibrosis: therapeutic insights from the small-molecule toolbox. Nat Rev Drug Discov 2015;14:693–720.
[29] Moeller A, Ask K, Warburton D, Gauldie J, Kolb M. The bleomycin animal model: a useful tool to investigate treatment options for idiopathic pulmonary fibrosis? Int J Biochem Cell Biol 2008;40:362–82.
[30] Konate K, Rydstrom A, Divita G, Deshayes S. Everything you always wanted to know about CADY-mediated siRNA delivery* (* but afraid to ask). Curr Pharm Des 2013; 19:2869–77.
[31] Poosti F, Bansal R, Yazdani S, Prakash J, Post E, Klok P, et al. Selective delivery of IFN-gamma to renal interstitial myofibroblasts: a novel strategy for the treatment of renal fibrosis. FASEB journal 2015;29:1029–42.
[32] Weng HL, Wang BE, Jia JD, Wu WF, Xian JZ, Mertens PR, et al. Effect of interferon-gamma on hepatic fibrosis in chronic hepatitis B virus infection: a randomized controlled study. Clinical gastroenterology and hepatology 2005;3:819–28.
[33] Zhou X, Lin W, Tan FK, Assassi S, Fritzler MJ, Guo X, et al. Decreased catalytic function with altered sumoylation of DNA topoisomerase I in the nuclei of scleroderma fibroblasts. Arthritis Res Ther 2011;13:R128.
[34] Allanore Y, Simms R, Distler O, Trojanowska M, Pope J, Denton CP, et al. Systemic sclerosis. Nat Rev Dis Primers 2015;1:15002.
[35] Fang F, Marangoni RG, Zhou X, Yang Y, Ye B, Shangguang A, et al. Toll-like Receptor 9 Signaling is Augmented in Systemic Sclerosis and Elicits Transforming Growth factor beta-Dependent Fibroblast Activation. Arthritis & rheumatology 2016;68: 1989–2002.
[36] Ding W, Pu W, Wang L, Jiang S, Zhou X, Tu W, et al. Genome-Wide DNA Methylation Analysis in Systemic Sclerosis reveals Hypomethylation of IFN-Associated Genes in CD4(+) and CD8(+) T Cells. J Invest Dermatol 2018;138:1069–77.
[37] Sangaletti S, Tripodo C, Cappetti B, Casalini P, Chiodoni C, Piconese S, et al. SPARC Oppositely Regulates Inflammation and Fibrosis in Bleomycin-Induced Lung damage. American Journal of Pathology 2011;179:3000–10.
[38] Wynn TA. Integrating mechanisms of pulmonary fibrosis. J Exp Med 2011;208: 1339–50.
[39] Wynn TA. Cellular and molecular mechanisms of fibrosis. J Pathol 2008;214: 199–210.
[40] Yoshizaki A, Yanaba K, Iwata Y, Komura K, Ogawa A, Akiyama Y, et al. Cell adhesion molecules regulate fibrotic process via Th1/Th2/Th17 cell balance in a bleomycin-induced scleroderma model. J Immunol 2010;185:2502–15.
[41] Wilson MS, Madala SK, Ramalingam TR, Gochuico BR, Rosas IO, Cheever AW, et al. Bleomycin and IL-1beta-mediated pulmonary fibrosis is IL-17A dependent. J Exp Med 2010;207:535–52.
[42] Rehli M, Niller HH, Ammon C, Langmann S, Schwarzfischer L, Andreesen R, et al. Transcriptional regulation of CHI3L1, a marker gene for late stages of macrophage differentiation. J Biol Chem 2003;278:44058–67.
[43] Takase H, Matsumoto K, Yamadera R, Kubota Y, Otsu A, Suzuki R, et al. Genome-wide identification of endothelial cell-enriched genes in the mouse embryo. Blood 2012; 120:914–23.
[44] Piera-Velazquez S, Mendoza FA, Jimenez SA. Endothelial to Mesenchymal transition (EndoMT) in the Pathogenesis of Human Fibrotic Diseases. Journal of clinical medicine 2016;5.
[45] Woodruff PG, Boushey HA, Dolganov GM, Barker CS, Yang YH, Donnelly S, et al. Genome-wide profiling identifies epithelial cell genes associated with asthma and with treatment response to corticosteroids. Proc Natl Acad Sci U S A 2007;104: 15858–63.
[46] Ye S, Eriksson P, Hamsten A, Kurkinen M, Humphries SE, Henney AM. Progression of coronary atherosclerosis is associated with a common genetic variant of the human stromelysin-1 promoter which results in reduced gene expression. J Biol Chem 1996;271:13055–60.
[47] Wei P, Yang Y, Guo X, Hei N, Lai S, Assassi S, et al. Identification of an Association of TNFAIP3 Polymorphisms with Matrix Metalloproteinase Expression in Fibroblasts in an Integrative Study of Systemic Sclerosis-Associated Genetic and Environmental Factors. Arthritis & rheumatology 2016;68:749–60.
[48] Depianto DJ, Chandriani S, Abbas AR, Jia G, N'Diaye EN, Caplazi P, et al. Heterogeneous gene expression signatures correspond to distinct lung pathologies and biomarkers of disease severity in idiopathic pulmonary fibrosis. Thorax 2015;70:48–55.